



# A Linear Transformation for the Reconstruction of the Responses of Systems in Similitude

Fiorella Tavasso<sup>1</sup> · Alessandro Casaburo<sup>2</sup> · Giuseppe Petrone<sup>1,2</sup> · Francesco Franco<sup>1,2</sup> · Sergio De Rosa<sup>1,2</sup>

Received: 21 December 2021 / Revised: 20 January 2022 / Accepted: 21 January 2022  
© The Author(s) 2022

## Abstract

Recent years have seen an increasing interest towards similitude methods. In fact, the possibility of testing a scaled model, instead of a full-scale prototype, leads to many advantages: financial and time savings, easier experimental setups, etc. However, similitudes have drawbacks, too, mainly due to non-scalable effects and partial similitude, which prevent from an accurate reconstruction of the prototype response. For these reasons, an alternative method which can bypass these limitations is needed. A new method, called VOODOO (Versatile Offset Operator for the Discrete Observation of Objects), is herein proposed: it is based on the definition of a transformation matrix which links the outputs of a given linear systems to those belonging to another system, which may be a scaled model. The responses are acquired on a discrete number of points for both the systems. This work aims at investigating the method's strengths and limitations of the method. The results show that, although VOODOO exhibits some lack of accuracy in off-design conditions due to the loss of spatial correlation, it is able to overcome some major restrictions that affect all similitude methods.

**Keywords** Similitude · Scaling laws · Linear transformation · Frequency response · Plate

## 1 Introduction

The use of similitudes has received a lot of attention in engineering field since analytical, numerical, and experimental analyses can be executed more easily in a transformed solution domain. In fact, by defining a set of similitude conditions and scaling laws, which allow to reconstruct the response of the full-scale prototype from that of a scaled model (and vice versa), it is possible to overcome many of the disadvantages characterizing experimental tests and numerical simulations, such as financial costs, set-up

management, computational power, etc. An example of the benefits and advantages of using scaled models of the original prototype are reported by Holmes and Sliter [7] which demonstrate how convenient it is, in both financial and temporal terms, to study the complex structural response of a conveniently scaled model of the various parts of the vehicle. Precisely, the authors estimate that in terms of cost there is a saving between 1/3 and 1/4 of the total cost of the real prototype and that in terms of time there is a reduction of about 1/3 of the time required for manufacturing and testing the prototype.

As reviewed in Casaburo et al [3] and Casaburo et al [4], structural similitudes prove to be useful in the investigation of many types of structures, as well as perform several types of analyses, concerning static and dynamic behavior, impact response, and failure analysis. For these purposes, several similitude methods have been proposed in literature. For example, Rezaeepazhand et al [10] apply STAGE (Similitude Theory Applied to Governing Equations) to predict the free vibrations and elastic buckling responses of laminated rectangular plates. Adams et al [1] derive sensitivity-based scaling laws, represented by power laws of the parameters characterizing the system under investigation; then, Luo et al [8] combine STAGE and sensitivity analysis to investigate

---

✉ Giuseppe Petrone  
giuseppe.petrone@unina.it

Alessandro Casaburo  
alessandro.casaburo@wavesetconsulting.com

Francesco Franco  
francof@unina.it

Sergio De Rosa  
derosa@unina.it

<sup>1</sup> Department of Industrial Engineering, University of Naples Federico II, Via Claudio 21, Naples 80125, Italy

<sup>2</sup> WaveSet S.R.L., Via A. Gramsci 15, Naples 80122, Italy

the dynamic similitude of thin-walled structures. Meruane et al [9] apply SAMSARA (Similitude and Asymptotic Models for Structural-Acoustic Research Applications) to perform a thorough numerical-experimental investigation on cantilever flexural plates; the same method is successfully applied by Berry et al [2] to analyse rectangular flexural orthotropic flat panels radiating sound. Other interesting works are proposed by Wang et al [11], that investigate the vibrations and sound radiation of underwater complex shell structures in similitude, Zhang et al [12], deriving scaling laws as weighted powers of scale factors through least squares method, and He et al [6] with the application of similitudes to an hybrid wave-coupled FE-SEA (Finite Element-Statistical Energy Analysis) method to predict the medium-frequency vibration response of a satellite solar array.

Similitudes and models can be classified in several ways; the most common approach is to define the type of similitude according to the parameters involved in the scaling procedure. This way, one can define:

- *Geometric similitude*: geometrical parameters are scaled, model and prototype are identical in shape but different in size.
- *Kinematic similitude*: kinematic parameters are scaled so that homologous particles are at homologous points in homologous times.
- *Dynamic similitude*: homologous parts of the model and prototype are subject to homologous net forces.

Another common way in which similitudes and models are classified depends on the fulfillment of a set of similitude conditions which are analytically derived. Particularly, it is possible to define:

- *True model*: all the similitude conditions are satisfied; the similitude is said to be complete.
- *Distorted model*: at least one of the similitude conditions is not satisfied. In this case, the similitude is partial. Sometimes, the model is also called avatar.

Despite the number of similitude methods formulated in recent decades, there are inevitably limitations in the applicability of the scaling laws. In fact, while a complete similitude makes it possible to accurately reconstruct the behaviour of the prototype, the partial similitude does not. Moreover, the derivation of similitude conditions and scaling laws becomes more convoluted as the system under investigation becomes more complex (laminated or sandwich structures, particular geometries, etc.). Nonetheless, the problem of partial similitudes (models which do not satisfy at least one similitude condition) must not be underestimated, since distortions are a true issue due to manufacturing errors and

limits. Therefore, there is a need to research and formulate alternative methods to overcome these drawbacks, which has led to the definition of VOODOO (Versatile Offset Operator for the Discrete Observation of Objects) method, already proposed in a work by De Rosa et al [5].

The purpose of this work is to investigate the performances of VOODOO in off-design conditions, with specific attention to single plates and assemblies of two plates. Thus, the article is structured as follows. Section 2 provides the theoretical basis underlying VOODOO method. Section 3 reports the results obtained when VOODOO is applied to three test cases. In particular, Sect. 3.1 deals with the application of VOODOO to two simply supported plates in design conditions and when one plate is excited in a point different from a VOODOO point; Sect. 3.2 concerns two assemblies of two plates in coplanar and orthogonal configuration; finally, in Sect. 3.3 a uniform pressure load is applied on a plate to investigate the performances of VOODOO. Section 4 draws the conclusions.

## 2 The VOODOO Method

The main purpose of VOODOO method is to estimate a linear transformation matrix  $\mathbf{T}$ , called VOODOO matrix, between the frequency response vectors of the prototype,  $\boldsymbol{\pi}(\omega)$ , and the model,  $\boldsymbol{\mu}(\omega)$  (where  $\omega$  is the angular frequency), both subjected to the same load.

For a given number  $N$  of excitation/acquisition points, equal for both the systems, if  $\mathbf{T}(\omega)$  is the frequency dependent transformation matrix between the two systems and if the output vector of the prototype is known, it is possible to derive the response of the model using the VOODOO matrix:

$$\boldsymbol{\mu}(\omega) = \mathbf{T}(\omega)\boldsymbol{\pi}(\omega). \tag{1}$$

Vice versa, the prototype response can be predicted from the model response; assuming  $\boldsymbol{\Theta}(\omega) = \mathbf{T}^{-1}(\omega)$ ,

$$\boldsymbol{\pi}(\omega) = \boldsymbol{\Theta}(\omega)\boldsymbol{\mu}(\omega). \tag{2}$$

The vectors  $\boldsymbol{\mu}(\omega)$  and  $\boldsymbol{\pi}(\omega)$  have size  $[N \times 1]$  and the matrix  $\mathbf{T}(\omega)$  and its inverse have size  $[N \times N]$ .

The VOODOO matrix is constructed as follows. A unit force ( $F_{\pi,1} = 1$ ) is applied to the first point of the prototype and the response of all  $N$  points ( $\boldsymbol{\pi}_1^{(F_{\pi,1}=1)}, \boldsymbol{\pi}_2^{(F_{\pi,1}=1)}, \dots, \boldsymbol{\pi}_N^{(F_{\pi,1}=1)}$ ) is derived. This procedure is repeated for the remaining  $N - 1$  points of the prototype. The same procedure is performed also for the model, applying the same load and obtaining the outputs  $\boldsymbol{\mu}_1^{(F_{\mu,i}=1)}, \boldsymbol{\mu}_2^{(F_{\mu,i}=1)}, \dots, \boldsymbol{\mu}_N^{(F_{\mu,i}=1)}$ , when the  $i$ -th point is excited. Once the responses of all prototype and model points to a unit force are evaluated,  $N$  linear systems can be written. For example, the first

system, due to the excitation of the first point of prototype and model, is given by

$$\begin{cases} \mu_1^{(F_{\mu,1}=1)} = T_{1,1}\pi_1^{(F_{\pi,1}=1)} + T_{1,2}\pi_2^{(F_{\pi,1}=1)} + \dots + T_{1,N}\pi_N^{(F_{\pi,1}=1)} \\ \mu_2^{(F_{\mu,1}=1)} = T_{2,1}\pi_1^{(F_{\pi,1}=1)} + T_{2,2}\pi_2^{(F_{\pi,1}=1)} + \dots + T_{2,N}\pi_N^{(F_{\pi,1}=1)} \\ \vdots \\ \mu_N^{(F_{\mu,1}=1)} = T_{N,1}\pi_1^{(F_{\pi,1}=1)} + T_{N,2}\pi_2^{(F_{\pi,1}=1)} + \dots + T_{N,N}\pi_N^{(F_{\pi,1}=1)} \end{cases} \tag{3}$$

The other  $N - 1$  systems can be written accordingly, considering that each one is due to the excitation of one point in both prototype and model. Hence, the last system, due to the excitation of the  $N$ -th point, is

$$\begin{cases} \mu_1^{(F_{\mu,N}=1)} = T_{1,1}\pi_1^{(F_{\pi,N}=1)} + T_{1,2}\pi_2^{(F_{\pi,N}=1)} + \dots + T_{1,N}\pi_N^{(F_{\pi,N}=1)} \\ \mu_2^{(F_{\mu,N}=1)} = T_{2,1}\pi_1^{(F_{\pi,N}=1)} + T_{2,2}\pi_2^{(F_{\pi,N}=1)} + \dots + T_{2,N}\pi_N^{(F_{\pi,N}=1)} \\ \vdots \\ \mu_N^{(F_{\mu,N}=1)} = T_{N,1}\pi_1^{(F_{\pi,N}=1)} + T_{N,2}\pi_2^{(F_{\pi,N}=1)} + \dots + T_{N,N}\pi_N^{(F_{\pi,N}=1)} \end{cases} \tag{4}$$

Equations 3–4 represent the outputs of the the model at each point, written as a linear combination of the output of the prototype and the elements  $T_{ij}$  of the VOODOO matrix, for a given frequency  $\omega$ . The points used for the determination of matrix  $\mathbf{T}$  are called VOODOO points. In this phase of construction of the VOODOO matrix, the VOODOO points coincide with the excitation/acquisition points.

To clarify, considering two panels, the prototype and a scaled-up model, and a number of points  $N = 4$ , the response of the latter at point 1 due to the excitation of point 3 (refer to Fig. 1) is given by

$$\mu_1^{(F_{\mu,3}=1)} = T_{1,1}\pi_1^{(F_{\pi,3}=1)} + T_{1,2}\pi_2^{(F_{\pi,3}=1)} + T_{1,3}\pi_3^{(F_{\pi,3}=1)} + T_{1,4}\pi_4^{(F_{\pi,3}=1)}, \tag{5}$$

which is a linear combination of the responses of the prototype due to the excitation of point 3 and measured in all the considered points.

Returning to the more general problem with  $N$  points, the  $N^2$  elements of the VOODOO matrix

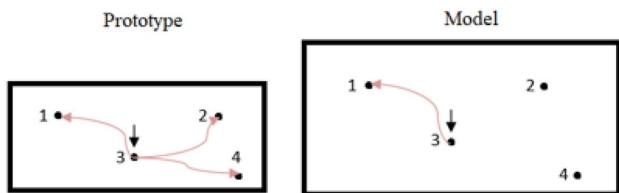


Fig. 1 Example of two panels in similitude with  $N = 4$ ; the black arrow indicates the excitation point, the red arrows the points used for the response evaluation

$$\mathbf{T} = \begin{bmatrix} T_{1,1} & T_{1,2} & \dots & T_{1,N} \\ T_{2,1} & T_{2,2} & \dots & T_{2,N} \\ \vdots & \vdots & \ddots & \vdots \\ T_{N,1} & T_{N,2} & \dots & T_{N,N} \end{bmatrix}. \tag{6}$$

are the unknown terms of the system.

Since Betti’s theorem and its extension, Maxwell’s theorem, state that in a linear elastic structure, the displacement at the  $i$ -th point, due to a unit force applied on the  $j$ -th point, is equal to the displacement at the  $j$ -th point due to a unit force acting at the  $i$ -th point. Hence, it is possible to write that

$$\mu_p^{(F_{\mu,q}=1)} = \mu_q^{(F_{\mu,p}=1)}, \tag{7}$$

as well as

$$\pi_p^{(F_{\mu,p}=1)} = \pi_q^{(F_{\mu,q}=1)}, \tag{8}$$

where  $p$  and  $q$  are two generic points of the systems.

This leads to

$$\begin{bmatrix} \pi_1^{(F_{\pi,1}=1)} & \pi_2^{(F_{\pi,1}=1)} & \dots & \pi_N^{(F_{\pi,1}=1)} \\ \text{symm} & \pi_2^{(F_{\pi,2}=1)} & \dots & \pi_N^{(F_{\pi,2}=1)} \\ \vdots & \vdots & \ddots & \vdots \\ \text{symm} & \text{symm} & \dots & \pi_N^{(F_{\pi,N}=1)} \end{bmatrix} \begin{bmatrix} T_{r,1} \\ T_{r,2} \\ \vdots \\ T_{r,N} \end{bmatrix} = \begin{bmatrix} \mu_r^{(F_{\mu,1}=1)} \\ \mu_r^{(F_{\mu,2}=1)} \\ \vdots \\ \mu_r^{(F_{\mu,N}=1)} \end{bmatrix}, \tag{9}$$

or, briefly,

$$\mathbf{\Gamma}\mathbf{T}^r = \boldsymbol{\mu}_r. \tag{10}$$

The columns of the matrix  $\mathbf{\Gamma}$  are the responses of the prototype to the unit load applied on each point. Thus, the  $i$ -th column of the matrix represents the response of the  $i$ -th point of the prototype to the unit load applied on each point. Each element of the matrix  $\mathbf{\Gamma}$  is known. The column vector  $\boldsymbol{\mu}_r$  is the response of the  $r$ -th point of the model to the unit load applied on each point. Each element of this vector is known, too. The column vector  $\mathbf{T}^r$  represents the  $r$ -th row of the unknown transformation matrix  $\mathbf{T}$ , which elements are, as stated before, unknown. Therefore they can be evaluated as

$$\mathbf{T}^r = \mathbf{\Gamma}^{-1}\boldsymbol{\mu}_r. \tag{11}$$

The term  $\mathbf{\Gamma}$  is a frequency-dependent matrix, containing the response of the prototype, which must be evaluated each time frequency sampling changes. Moreover, the design of the VOODOO matrix  $\mathbf{T}$  is based on the outputs of the points to a unit excitation applied to each point, therefore material properties, damping, and boundary conditions are indirectly taken into account.

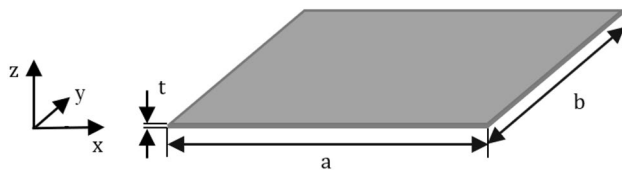


Fig. 2 Plate geometrical characteristics

Table 1 Geometrical characteristics of prototype and model

Model	Length, a [m]	Width, b [m]	Thickness, t [m]
Prototype	0.656	0.400	0.001
Model	0.460	0.364	0.003

Table 2 Material properties of prototype and model (aluminium)

Young's modulus, E [Pa]	$71 \times 10^9$
Mass density [kg/m <sup>3</sup> ], $\rho$	2723
Poisson's ratio, $\nu$	0.33
Prototype damping, $\eta_\pi$	0.01
Model damping, $\eta_\mu$	0.005

### 3 Validation of VOODOO Method

In this section, VOODOO method is applied to investigate its reliability in off-design conditions. Three test cases are presented. The first case concerns two simply supported plates excited by a concentrated force in which the excitation point does not coincide with any of the VOODOO points. Secondly, two assemblies of two plates, with coplanar and orthogonal arrangements, are investigated. Finally, two simply supported plates subjected to a pressure load are analysed. All applications of VOODOO involve the reconstruction of the model response from that of the prototype; moreover, all the responses are local, not averaged, since the method is meant to work with local responses.

#### 3.1 Test Case 1: Two Simply Supported Plates

The first validation test of the VOODOO method concerns two plates in partial similitude, the prototype and a distorted model, which geometrical and material properties are summarized in Tables 1–2, are simply supported. Three VOODOO points are used for the construction of the

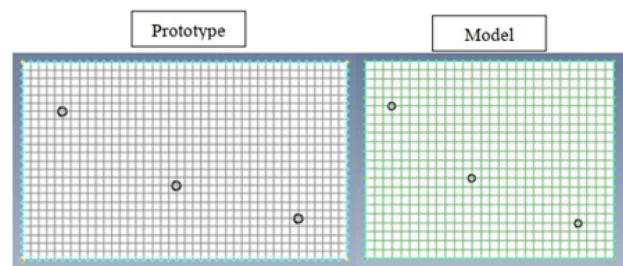


Fig. 3 VOODOO points of both prototype and model in test case 1

Table 3 Dimensionless coordinates of prototype VOODOO points in test case 1

Point number	x/a	y/b
Point 1	0.125	0.856
Point 2	0.475	0.428
Point 3	0.850	0.106

Table 4 Dimensionless coordinates of model VOODOO points in test case 1

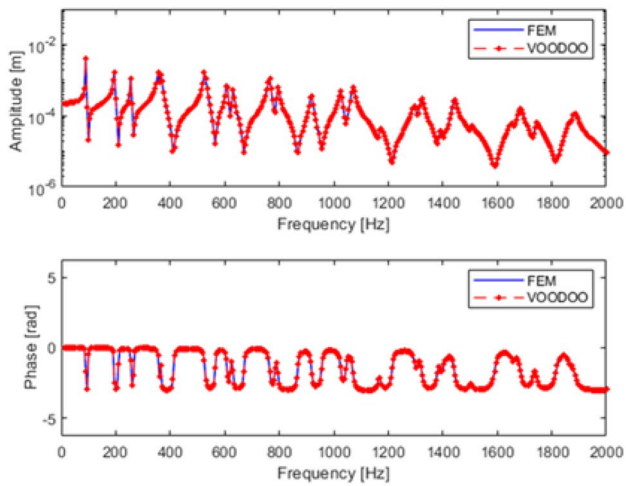
Point number	x/a	y/b
Point 1	0.208	0.771
Point 2	0.375	0.406
Point 3	0.750	0.181

transformation matrix; they are shown in Fig. 3 and their dimensionless coordinates are listed in Tables 3–4. The geometrical characteristics of a plate are shown in Fig. 2.

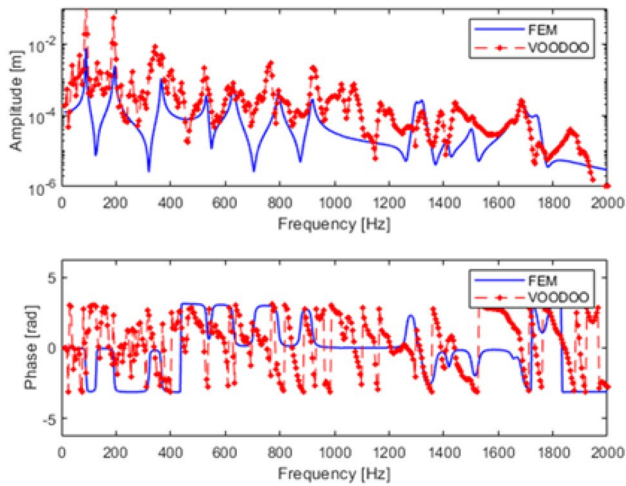
To construct the VOODOO matrix, which is different for each frequency, the frequency range (and the number of spectral lines) considered for the FRF analysis is the same for both prototype and model, namely a [0–2000] Hz range, with a frequency resolution equal to 5 Hz.

The VOODOO transformation matrix is constructed for each frequency. A three-dimensional matrix  $[N \times N] \times N_f$  is created, where  $N_f$  represents the number of used frequency points.

A first validation test is performed considering the same systems used to derive the VOODOO matrix, both subjected to a concentrated load  $F$  equal to 100 N. The results are shown in Fig. 4, displaying the reconstruction of the model displacement from that of the prototype in terms of amplitude and phase in two different situations. Namely, Fig. 4a shows the results when the excitation and acquisition points coincide with the VOODOO points (i.e., Point 1). The plots exhibit a perfect overlap between the reference and predicted curves. This is due to the fact that the reconstruction is applied to points directly involved into the VOODOO matrix, therefore the transformation is built *ad hoc* for such a



(a)



(b)

**Fig. 4** Amplitude and phase of model’s Point 1 displacement, when (a) the excitation points coincide with the VOODOO points, and (b) the excitation point does not coincide with any of the VOODOO points

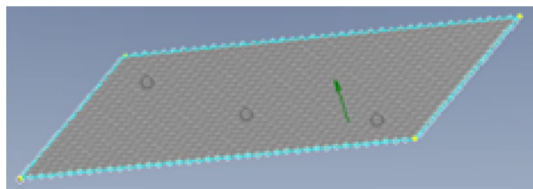
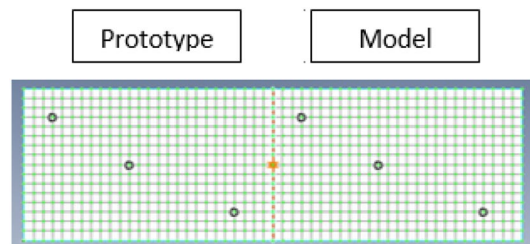


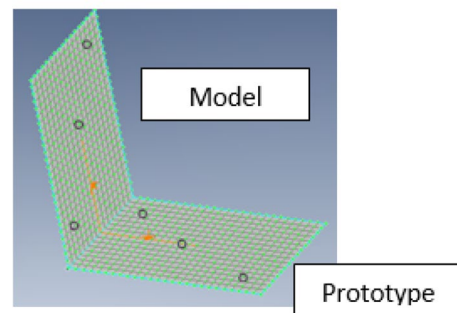
**Fig. 5** Model VOODOO points; the green arrow indicates the new excitation point, different from the VOODOO points

configuration. The same accuracy can be obtained when the behavior of the prototype is derived from that of the model De Rosa et al [5].

Instead, Fig. 4b shows the results obtained when the structure is not excited in a VOODOO point. The new excitation point is shown in Fig. 5, and has dimensionless coordinates (0.774, 0.208). Even though the first resonance peaks are well predicted, which is of no little significance when dealing with systems in partial similitude, the amplitudes are not well reconstructed: since there is no spatial correspondence between the VOODOO points and the excitation point, the prediction is not as accurate as in the previous case. Thus, the method is sensitive to the switch of a VOODOO point with another, generic point when it is used for exciting the system. Such a drawback may be overcome by increasing the number of VOODOO points: on the one hand, this approach would lead to bigger matrices, thus to procedures more computationally expensive; on the other hand, a thorough distribution of several VOODOO points may help to bound amplitude shifts, like those shown in Fig. 4b, when predicting the responses De Rosa et al [5]. In fact, any excitation point would be closer to a VOODOO point with respect to the case with fewer points.



(a)



(b)

**Fig. 6** Plates configurations for test case 2, namely (a) coplanar and (b) orthogonal

**Table 5** Dimensionless coordinates of prototype and model VOODOO points in both the coplanar and orthogonal configurations of test case 2

	$x/a$	$y/b$
<b>Point 1</b>	0.114	0.812
<b>Point 2</b>	0.422	0.500
<b>Point 3</b>	0.846	0.187

### 3.2 Test Case 2: Assembly of Two Plates

The test case 2 concerns two joined panels in two different configurations: coplanar and orthogonal, like shown in Figs. 6a–6b, respectively. Thus, this test case addresses the problem of peculiar geometrical distributions of VOODOO points. The plates sizes do not change with respect to test case 1, they are simply joined together. Therefore, in this part of the work there are no more two plates in similitude, but two plates joined so that they compose an assembly. However, the reference plate is still called prototype, as well as the other plate is called model. Concerning the coplanar plates, the prototype is the left one and the model is the right one. They are joined along the prototype's right side and the model's right side.

For both the assemblies a frequency range of [0–1000] Hz is chosen for the analysis. Table 5 summarizes the dimensionless coordinates of VOODOO points, for both the prototype and model, of the coplanar and orthogonal configurations, respectively. Both prototype and model have the same VOODOO points dimensionless coordinates, as well as both the assemblies. However, in the orthogonal configuration, the points of the vertical plates have  $(y, z)$  coordinates. To avoid any ambiguity in the nomenclature, for this plate a local reference frame is considered by rotating around the  $y$  axis, which remains the same, so that the local  $x$  axis, used to describe the position of the VOODOO points, is coincident with the global  $z$  axis. With this reference frames in mind, the prototype is the plate in the global  $xy$  plane, the model is the plate in the global  $yz$  plane.

In both the configurations, the VOODOO matrix is constructed by exciting only the prototype and acquiring the response in both the prototype and model. For validation, a concentrated force  $F$  equal to 150 N is applied to the prototype.

Figure 7 shows the response predictions provided by VOODOO for all the acquisition points of the model (coinciding with the VOODOO points) when the Point 2 of the prototype is excited. In particular, Figs. 7a–7c display the displacement amplitude and phase of model's Points 1–3, respectively, when Point 2 of the prototype is excited. The only case in which the spatial correspondence is retained is the one illustrated in Fig. 7b, that is, Point 2 of the model. Therefore, this is the only case in which the reconstruction is satisfactory.

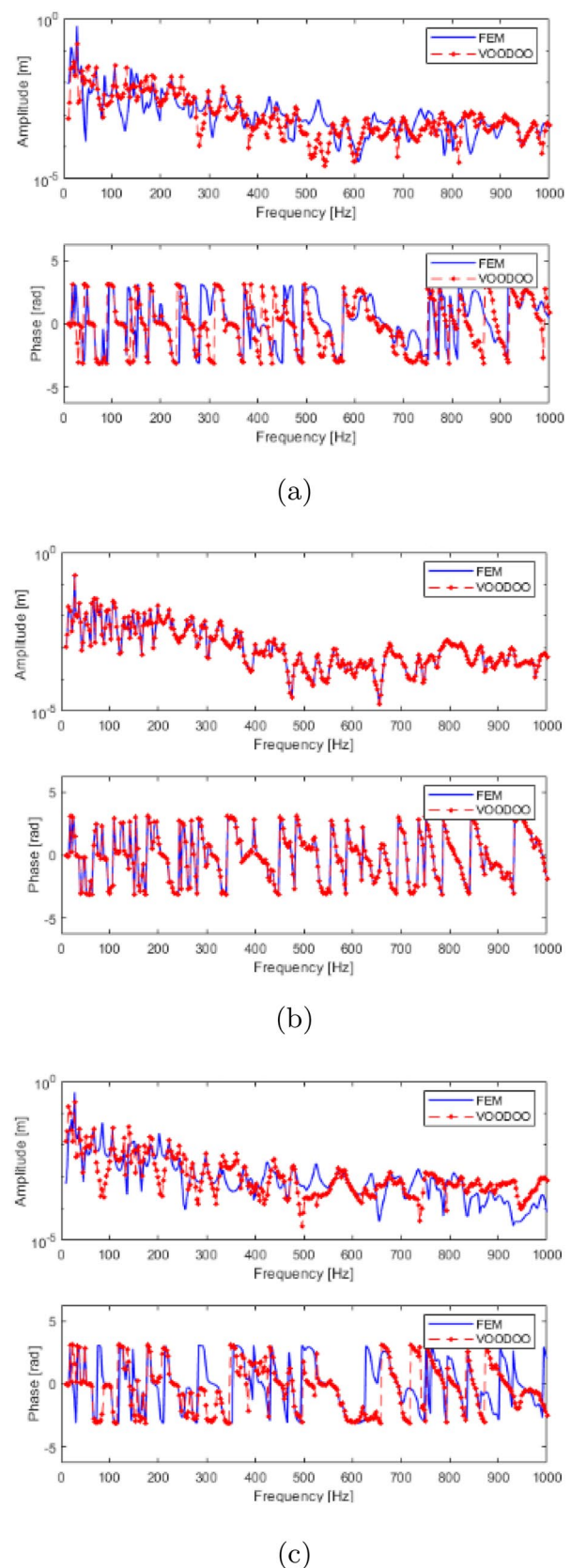


**Fig. 7** Amplitude and phase of model's Point (a) 1, (b) 2, and (c) 3, when Point 2 of the prototype is excited. Coplanar configuration

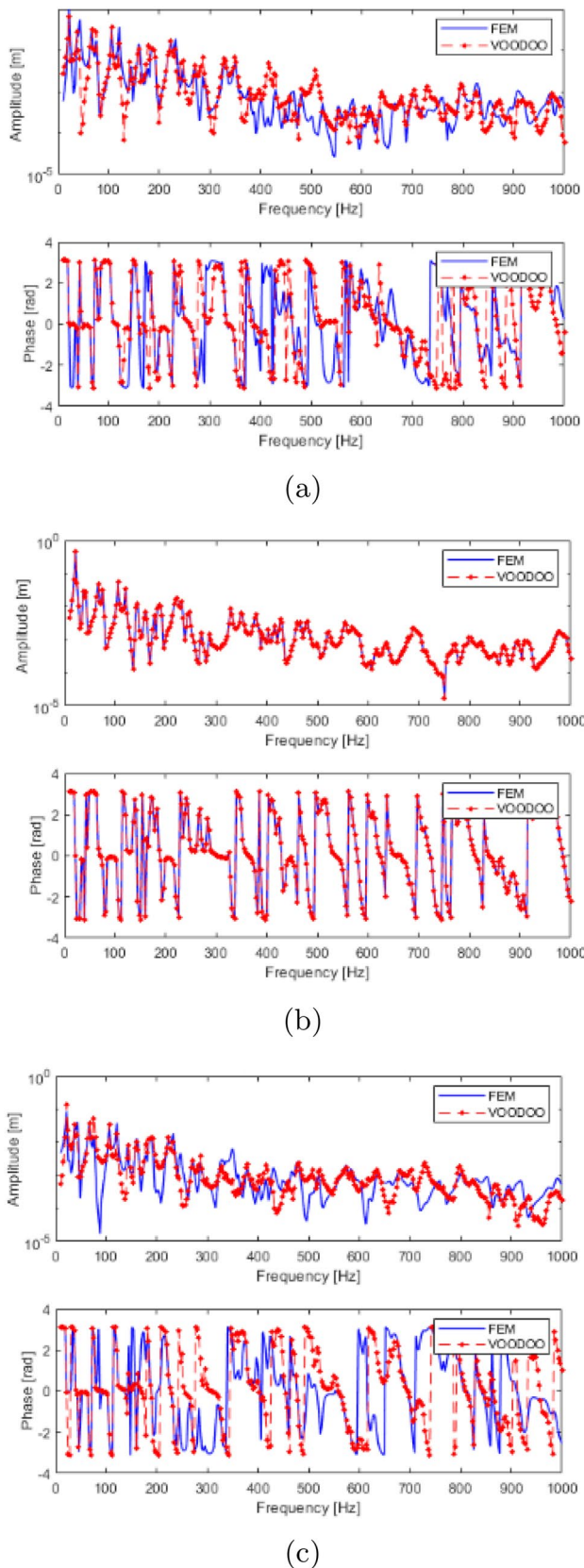


Fig. 8 Amplitude and phase of model's Point (a) 1, (b) 2, and (c) 3, when Point 2 of the prototype is excited. Orthogonal configuration

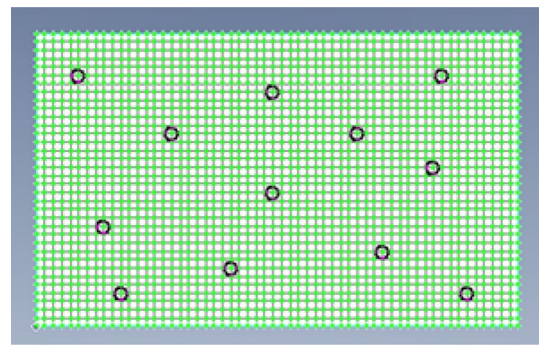


Fig. 9 VOODOO points of the prototype when a pressure load is applied

The same results are obtained when the two panels are arranged orthogonally, as Fig. 8 shows. Hence, the different orientation of a plate with respect to the other does not affect not only the reconstruction process, but also the application of the method itself.

In this case, the same considerations made for the coplanar assembly hold.

### 3.3 Test Case 3: Two Simply Supported Plates Subjected to a Uniformly Distributed Pressure Load

The simply supported plates used in test case 1 are herein used in order to investigate the potentialities of VOODOO when a pressure load excites the test articles. Twelve VOODOO points are used, indicated in Fig. 9 (the dimensionless coordinates are reported in Appendix A) only for the prototype, since they are the same for the model. The increase of the density of VOODOO points is used in the attempt to reduce the discrepancies between the prototype and model reconstructed responses introduced by the pressure load, which is applied not only on the VOODOO points, but also in all the other points of the plate. Therefore, while the excitation of the original VOODOO points may assure an accurate prediction of the displacements, the involvement of all other points may introduce disturbances when the transformation matrix is applied.

After the typical construction of VOODOO matrix, to reproduce a pressure load in the test phase, a set of local forces with the same magnitude are applied on all the points of the plate. In particular, the prototype is loaded with a set of forces so that the pressure distribution is constant on the entire plate and equal to 1 Pa.

Figure 10 shows the reconstruction provided by VOODOO for point 3 of the model. Also in this case, the prediction is not accurate. In fact, since all the points of the model are excited, the spatial correlation between VOODOO, excitation, and acquisition points is not retained.

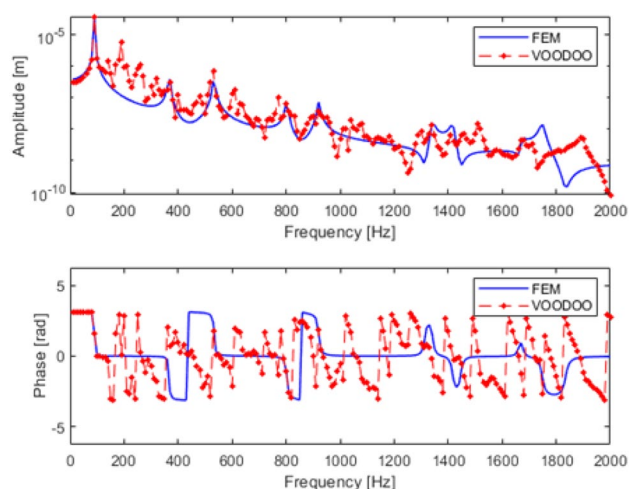


**Fig. 10** VOODOO reconstruction of model's Point 3 when a pressure load is applied

## 4 Conclusions

This article shows new applications of VOODOO method, highlighting its potentialities and limits at this stage of development. In particular, it is applied to several off-design conditions: when the plate is excited in a point which is different from a VOODOO point, when the plates are joined with a coplanar and an orthogonal assembly, and when the plate is loaded with a uniform pressure. When VOODOO is applied in off-design conditions, its predictions are not as accurate as the design conditions, mainly because the spatial correlation between the excitation/acquisition and VOODOO points is lost. However, VOODOO proves to be a simple and immediate method to apply, since only the structural responses must be provided in order to generate the VOODOO matrix. Moreover, its potentialities are wide, since several types of structures can be investigated and linked through the transformation matrix, which makes VOODOO an advantageous method in several engineering fields. Therefore, further research should focus on improving the method when off-design conditions are considered, for example by involving similitude methods, since considering excitation/acquisition points different from VOODOO points may be seen as considering distorted similitudes [3], or particular shape functions which may transmit the response information among structures with different size.

## Appendix: Test Case 3 Dimensionless Coordinates

Tables 6–7 report the dimensionless coordinates of VOODOO points used in test case 3, Sect. 3.3, for prototype and model, respectively.

**Table 6** Dimensionless coordinates of prototype VOODOO points in test case 3

	x/a	y/b
<b>Point 1</b>	0.175	0.112
<b>Point 2</b>	0.893	0.112
<b>Point 3</b>	0.402	0.200
<b>Point 4</b>	0.717	0.255
<b>Point 5</b>	0.140	0.342
<b>Point 6</b>	0.490	0.455
<b>Point 7</b>	0.823	0.542
<b>Point 8</b>	0.280	0.655
<b>Point 9</b>	0.666	0.655
<b>Point 10</b>	0.490	0.800
<b>Point 11</b>	0.086	0.855
<b>Point 12</b>	0.841	0.855

**Table 7** Dimensionless coordinates of model VOODOO points in test case 3

	x/a	y/b
<b>Point 1</b>	0.200	0.060
<b>Point 2</b>	0.850	0.093
<b>Point 3</b>	0.423	0.153
<b>Point 4</b>	0.700	0.217
<b>Point 5</b>	0.150	0.280
<b>Point 6</b>	0.500	0.436
<b>Point 7</b>	0.800	0.467
<b>Point 8</b>	0.323	0.623
<b>Point 9</b>	0.650	0.623
<b>Point 10</b>	0.500	0.780
<b>Point 11</b>	0.100	0.843
<b>Point 12</b>	0.850	0.873

## Declarations

**Conflict of interest** On behalf of all authors, the corresponding author states that there is no conflict of interest.

**Open Access** This article is licensed under a Creative Commons Attribution 4.0 International License, which permits use, sharing, adaptation, distribution and reproduction in any medium or format, as long as you give appropriate credit to the original author(s) and the source, provide a link to the Creative Commons licence, and indicate if changes were made. The images or other third party material in this article are included in the article's Creative Commons licence, unless indicated otherwise in a credit line to the material. If material is not included in the article's Creative Commons licence and your intended use is not permitted by statutory regulation or exceeds the permitted use, you will need to obtain permission directly from the copyright holder. To view a copy of this licence, visit <http://creativecommons.org/licenses/by/4.0/>.

## References

- Adams, C., Bös, J., Slomski, E.M., et al.: Scaling laws obtained from a sensitivity analysis and applied to thin vibrating structures. *Mech. Syst. Signal Process.* **110**, 590–610 (2018)



2. Berry, A., Robin, O., Franco, F., et al.: Similitude laws for the sound radiation of flat orthotropic flexural panels. *J. Sound Vib.* **489**, (2020). <https://doi.org/10.1016/j.jsv.2020.115636>
3. Casaburo, A., Petrone, G., Franco, F., et al. A review of similitude methods for structural engineering. *Appl. Mech. Revi.* 71(3) (2019). <https://doi.org/10.1115/1.4043787>
4. Casaburo, A., Petrone, G., Franco, F., et al. Similitude theory applied to plates in vibroacoustic field: a review up to 2020. *Progress in Scale Modeling, and International Journal* 1:1–13. (2020) <https://doi.org/10.13023/psmij.2020.03>
5. De Rosa, S., Franco, F., Petrone, G., et al.: A versatile offset operator for the discrete observation of objects. *J. Sound Vib.* **500**, (2021). <https://doi.org/10.1016/j.jsv.2021.116019>
6. He, F., Luo, Z., Li, L., et al.: A similitude for the middle-frequency vibration response of satellite solar array based on the wave coupling hybrid finite element-statistical energy analysis method. *Proc. Inst. Mech. Eng. Part C* **234**(18), 3560–3570 (2020)
7. Holmes, B.S., Sliter, G.: *Scale Modeling of Vehicle Crashes—Techniques, Applicability, and Accuracy; Cost Effectiveness*, p. 740586. Tech. Rep, SAE paper no (1974)
8. Luo, Z., Wang, Y., Zhu, Y., et al.: The dynamic similitude design method of thin walled structures and experimental validation. *Shock Vib.* **2016**, 1–11 (2016)
9. Meruane, V., De Rosa, S., Franco, F.: Numerical and experimental results for the frequency response of plates in similitude. *Proc Inst Mech Eng Part C* **230**(18), 3212–3221 (2015). <https://doi.org/10.1177/0954406215610148>
10. Rezaeepazhand, J., Simitse, G.J., Starnes, J.H., Jr.: Use of scaled-down models for predicting vibration response of laminated plates. *Composite Struct* **30**, 419–426 (1995)
11. Wang, S., Yang, G., Liu, N.: Investigation of acoustic scale effects and boundary effects for the similitude model of underwater complex shell structure. *J. Mar. Sci. Appl.* **6**(1), 31–35 (2007)
12. Zhang, W., Luo, Z., Zhang, W.D., et al.: Determination method of scaling laws based on least square method and applied to rectangular thin plates and rotor-bearing systems. *Mech. Based Design Struct. Mach.* **48**(2), 241–265 (2019)

**Publisher's Note** Springer Nature remains neutral with regard to jurisdictional claims in published maps and institutional affiliations.